Physiol Genomics 23: 46–53, 2005.
First published June 7, 2005; 10.1152/physiolgenomics.00077.2005.

A physiogenomic approach to study the regulation of blood pressure

Timm H. Westhoff,[1] Stefanie Scheid,[2] Markus Tölle,[1] Bogac Kaynak,[2] Sven Schmidt,[1] Walter Zidek,[1] Silke Sperling,[2,*] and Markus van der Giet[1,*]

[1]*Medizinische Klinik IV, Nephrology, Charité, Campus Benamin Franklin, and* [2]*Max Planck Institute for Molecular Genetics, Berlin, Germany*

Submitted 31 March 2005; accepted in final form 2 June 2005

Westhoff, Timm H., Stefanie Scheid, Markus Tölle, Bogac Kaynak, Sven Schmidt, Walter Zidek, Silke Sperling, and Markus van der Giet. A physiogenomic approach to study the regulation of blood pressure. *Physiol Genomics* 23: 46–53, 2005. First published June 7, 2005; 10.1152/physiolgenomics.00077.2005.—Several vasoregulatory systems including the renin-angiotensin system, sympathetic vasoregulation, and cytokine release have been studied extensively. The aim of the present study was to establish a physiogenomic screening model for differentially expressed genes in the regulation of blood pressure that might give a hint as to new vasoregulatory mechanisms. We induced acute hypotension in normotensive rats, assuming that vasoregulatory systems will counteract hypotension. Microarray transcriptome analysis was performed from kidneys 6 h after the induction of acute hypotension. The results were confirmed by real-time PCR. Six functionally known genes (*Igfbp1*, *Xdh*, *Sult1a1*, *Mawbp*, *Por*, and *Gstm1*) and two expressed sequence tages (*BI277460* and *AI411345*) were significantly upregulated. Four of these genes (*Igfbp1, Xdh, Por,* and *Gstm1*) have well-characterized functions in the cardiovascular system. The proteins corresponding to *Xdh*, *Por*, and *Gstm1* are involved in the metabolism of reactive oxygen species (ROS). Because ROS can mediate endothelial dysfunction, we measured the aortic dilatory capacity in thoracic aortic rings. Indeed, vasodilator potency to acetylcholine was largely diminished in hypotensive animals, whereas sodium nitroprusside induced equivalent vasodilations in normotensive and hypotensive animals. The vasodilator potency of the endothelium was partially restored by the superoxide scavenger tiron. Hence, acute hypotension induces a diminished vasodilator potency of the endothelium due to an accelerated degradation of nitric oxide by ROS. The present physiogenomic approach is capable of detecting vasoregulatory mechanisms and may provide deeper insight into the genetics and physiology of blood pressure regulation.

geneticsendotheliummicroarrayreactive oxygen species

VASCULAR TONE is regulated by a dynamic balance of local chemical, neural, and humoral mechanisms. The systemic regulatory mechanisms synergize with local mechanisms and adjust specific vascular responses in different vascular beds. Because of its central role in volume and vascular resistance regulation (e.g., the renin-angiotensin-aldosterone system), the kidney constitutes a major component in the systemic control of blood pressure (35). Local control of blood pressure is largely affected by chemical conditions (pH, O_2 tension, and CO_2 tension) and the paracrine properties of the endothelium. The vascular endothelium releases several vasodilator and vasoconstrictor substances including prostaglandins, thromboxanes, nitric oxide (NO), endothelins, complex nucleotides, and reactive oxygen species (ROS) (17, 29, 40). At present, there is increasing evidence that vascular cytochrome *P*-450 metabolites of arachidonic acid (20-hydroxyeicosatetraenoic acid and epoxyeicosatrienoic acid) play an important role in the control of vascular tone and in the long-term control of arterial blood pressure (23). Thus a broad variety of vasoactive factors have been depicted, but the underlying genetic regulatory mechanisms remain elusive.

The aim of the present study was to establish a model that gives an opportunity to identify new blood pressure regulating genes and their effects on vascular endothelial function. A decrease in blood pressure induces the release of counteracting vasoconstrictor agents or the suppression of vasodilator substances. We hypothesized that some of these processes are mediated by differential gene expression and established a rodent model with acute hypotension that allows a microarray-based large-scale screening for compensatorily regulated genes. We identified differentially expressed genes involved in a reduced endothelial bioavailability of NO, and we showed that acute hypotension induces an endothelial response resembling the condition generally referred to as "endothelial dysfunction."

METHODS

Animal experimental procedures. Ten 12-wk-old male Wistar-Kyoto (WKY) rats (220–250 g, Charles River Laboratories) were maintained in a room controlled at a temperature of 24 ± 2°C and relative humidity of 40–70% and given food and water ad libitum. Animals were randomly assigned to two groups. To induce acute hypotension, 3 ml of blood were withdrawn in five animals by ventricular punction, whereas the control rats underwent ventricular punction without bleeding. All procedures were carried out under ether anesthesia as described by Dietz and coworkers (4). Systolic blood pressure was measured by the tail-cuff method according to Bunag (1) before (−0.5 h) and after blood withdrawal (0, 3, and 6 h); 6 h after ventricular punction, the kidneys were removed, snap frozen in liquid nitrogen, and stored at −80°C until use. For arterial relaxation studies, the thoracic aorta was excised carefully, and a 2-mm aortic ring was mounted in a myograph immediately. The remaining aortic tissue was snap frozen in liquid nitrogen and stored at −80°C until use for real-time PCR. The animal experimental protocol was approved by the Ethics Review Committee for Animal Experimentation (Berlin, Germany). All procedures adhered to principles stated in the *Guide for the Care and Use of Laboratory Animals* by the German Society of Physiology.

Microarray analysis. Kidney samples were homogenized, and total RNA was obtained using TRIzol reagent (GIBCO-BRL) according to the manufacturer's protocol. RNA was purified on an affinity resin (RNeasy, Qiagen). Double-stranded cDNA was synthesized from 5 μg total RNA using the Superscript Choice System (Invitrogen) with an oligo-dT primer containing a T7 promoter sequence (TibMolBiol).

* S. Sperling and M. van der Giet contributed equally to this work.

Article published online before print. See web site for date of publication (http://physiolgenomics.physiology.org).

Address for reprint requests and other correspondence: M. van der Giet, Charité, Campus Benjamin Franklin, Medizinische Klinik IV, Nephrologie, Hindenburgdamm 30, 12200 Berlin, Germany (E-mail: markus.vandergiet@charite.de)

Biotin-labeled cRNA was obtained from the cDNA by in vitro transcription with a T7 RNA polymerase using the BioArray RNA Transcript Labeling Kit (Enzo Diagnostics). cRNA probe samples were purified by column cleanup using an RNeasy minikit (Qiagen). After quantification of the cRNA concentration, cRNA was fragmented and hybridized at 45°C for 16 h to an Affymetrix rat genome 230A array containing 15,923 probe sets (Affymetrix). The arrays were washed, stained, and scanned using a Fluidics Station and microarray scanner, which are components of the Affymetrix GeneChip Instrument System (Affymetrix). The microarray data were prepared according to minimum information about a microarray experiment (MAIME) recommendations, have been submitted to theGene Expression Omnibus (GEO) database, and can be accessed at http://www.ncbi.blm.bih.gov/geo. The GEO accession number for the corresponding platform is GSE2401. Data of the nine arrays can be retrieved with GEO accession numbers GSM45188, GSM45190, GSM45191, and GSM45192 (hypotension) and GSM45184, GSM45186, GSM45187, and GSM45193 (normotension).

Statistical analysis of microarray results. For data analysis we used the open source software R together with its bioinformatics packages collected in the Bioconductor project (10, 14). Software R is freely available from http://www.r-project.org, and Bioconductor is freely available from http://www.bioconductor.org.

After individual background correction with package "affy," the set of nine microarrays was normalized on probe level using the variance-stabilizing method in the package "vsn" (13). Within-probe set summarization (15) returned 15,923 expression values/chip. These two steps resulted in expression values on an additive scale that approximates the logarithmic scale. Hence, when "fold changes" are reported, these are exponentials of log ratios. Using the package "twilight," each gene was tested for differential expression between case and control samples by calculating the *Z* score (6). Statistical significance was assessed in a permutation test where *Z* scores under all possible combinations of the vector of condition labels were computed. The numbers of 4 case versus 5 control samples lead to 126 possible permutations including the original order. For each gene, all permutation *Z* scores were computed and summarized in an empirical *P* value that is the proportion of absolute permutation *Z* scores being equal or larger than the absolute *Z* score of the original vector.

The false discovery rate (FDR) was computed using the package "siggenes," which reimplements popular significance analysis of microarrays (SAM) software (39). The SAM method to estimate the FDR of a set of genes is based on the difference between observed and expected scores. That is, a gene is called differentially expressed if the difference of its observed to the corresponding expected score exceeds a certain threshold.

Real-time PCR. Total RNA was isolated, and cDNA was synthetized from kidney and aorta samples as described above. Real-time PCR assays were carried out using SYBR green PCR Master Mix (Applied Biosystems) on a GeneAmp 5700 Sequence Detection System (Applied Biosystems) according to the manufacturer's protocol. Intron spanning primers (TibMolBiol) were designed using Primer Express software (Applied Biosystems) and are presented in Table 1. RR was performed with avian myeloblastosis virus (AMV) reverse transcriptase (Promega), random hexamers, (Amersham Pharmacia Biotech), and 1 μg total RNA. We analyzed the significance of the normalized$\Delta\Delta C_T$ values with *t*-tests (where C_T is cycle threshold). Because of the small number of samples, we considered genes with $P < 0.1$ as confirmed to be differentially expressed. Data normalization was performed using the gene for β-actin as a housekeeping gene.

Arterial relaxation studies. The endothelial function of hypotensive and normotensive animals was evaluated in 2-mm rings of thoracic aortae that were mounted in a small vessel myograph. For reasons of comparability, rings of both groups were tested simultaneously in the same chamber. The wall tension of the vasculature was measured using established methodology (26). After equilibration and submaximal precontraction with phenylephrine (PE; 1 μmol/l), relaxation to 1 nmol/l–100 μmol/l acetylcholine (ACh) was tested. The maintenance of functional smooth muscle cell integrity after manipulation was confirmed by evaluation of endothelium-independent relaxation to sodium nitroprusside (SNP; 1 μmol/l). After being washed, rings were contracted with PE again, and the effects of ACh and SNP were reassessed in the presence of the superoxide scavenger tiron (1 mmol/l). Data are presented as means ± SE. Statistical analysis was performed with the Mann-Whitney test, and dose-response curves were compared using Friedman's test. All *P* values presented are two tailed. *P* values <0.05 were considered to be significant. Similar experiments were performed in isolated perfused kidneys of these rats but turned out to be much less reproducible than those done in aortae. Therefore, in the following, the findings in aortae are described.

Table 1. *Primer sequences used for real-time PCR*

Gene	Primer
Igfbp1	
Forward	5′-TCAAGAAATGGAAGGAGCCCT-3′
Reverse	5′-TCTCCTGCTTTCTGTTGAGCG-3′
Xdh	
Forward	5′-AGGGAATCTCCTTCGGAGCTT-3′
Reverse	5′-TTTAGCAATCTCCTCCGCCA-3′
Sult1a1	
Forward	5′-CAAGGTGATCTACATTGCCCG-3′
Reverse	5′-TGCAGCTTGGCCATGTTGT-3′
Mawbp	
Forward	5′-CCCCAGGACTTCCATGAAGTT-3′
Reverse	5′-ATAAGAATCGCTGAGCCGGAC-3′
Por	
Forward	5′-TCAGCAAGATCCAAACAACGG-3′
Reverse	5′-CCACGAAGCTGCTCTCTTTGA-3′
Gstm1	
Forward	5′-ACGCTCCCGACTATGACAGAA-3′
Reverse	5′-AAGTCCAGGCCCAGTTTGAAC-3′
BI277460	
Forward	5′-TATGACAACTGTTGGCTGGCTC-3′
Reverse	5′-GCTCTTGGGTAATGATGACCGT-3′
AI411345	
Forward	5′-GACGGAACGGTGTTTGAGATC-3′
Reverse	5′-GCACTCTGTGTTCGTTCTGCA-3′
LOC286921	
Forward	5′-CAAGAAAACCACAGCCCAGGT-3′
Reverse	5′-CACGTTCCTCTGGATGTGGAA-3′
BM386079	
Forward	5′-AGGACTCCAGCAACGACTTGTC-3′
Reverse	5′-CTGAGCTGCATACTGGATGACC-3′
BF400606	
Forward	5′-CGCTATAAGTGCAGTGTGTGCC-3′
Reverse	5′-GAAGCTATCAGAGAGGTGGCCA-3′
BE329273	
Forward	5′-TGGTGTCTGCATGACCAACTG-3′
Reverse	5′-AAATGTAGGTCTTGCCCCTGG-3′

RESULTS

To induce a significant counterregulation, we intended a 30% decrease of systolic blood pressure by bleeding. In preliminary experiments, the blood volume required was determined to be 3 ml for 240- to 250-g animals. In the present study, 3 ml blood withdrawal evoked a significant decrease ($P < 0.05$) of systolic pressure by 31 ± 5% of maximum systolic blood pressure ($n = 5$). When the organs were removed (6 h), systolic pressure had recovered to 87 ± 2% of baseline but was still significantly lower ($P < 0.05$) than that in the normovolemic group. The blood pressure changes before and after bleeding are presented in Fig. 1.

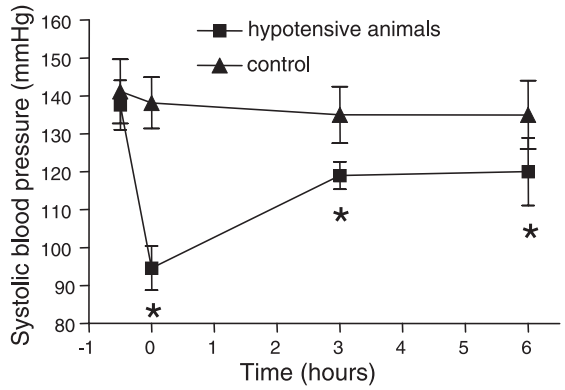

Fig. 1. Blood pressure in hypotensive and control animals after withdrawal of 3 ml blood. Changes in blood pressure are presented before (−0.5 h) and after bleeding (0, 3, and 6 h). *$P < 0.05$, significant difference of blood pressure versus control animals ($n = 5$).

Table 2. *Number of significantly differentially expressed genes in the microarray analysis*

Coverage of Confidence Interval, %	Number of Significant Genes	Estimated FDR
99.9	1	0
97.5	2	0
97.0	3	0
95.0	4	0
89.0	12	0
75.0	23	0
60.0	36	0
25.0	59	0.0314
5.5	124	0.0933

Numbers of significant genes and corresponding estimated false discovery rates (FDR) for various choices of confidence intervals for the absolute difference between observed and expected Z scores are shown. The first column contains the percentage that is covered by the confidence interval.

To examine whether acute hypotension induces a counteracting transcriptional regulation process, we carried out a transcriptome analysis in kidneys. Microarray test hybridizations revealed adequate signals for 9 of 10 cRNA samples, which were used for further analysis.

To test for differential gene expression between the hypotensive and control groups, we calculated the Z score. Figure 2 shows a scatterplot where the sorted observed Z scores are plotted against their "expected" Z scores obtained through permutations. Scores exceeding the marked 89% confidence intervals represent 12 highly significantly differentially expressed genes. A closer inspection reveals that the observed scores deviate from the expected ones much more at the upper end. Hence, we observed significantly upregulated genes but no significant downregulation.

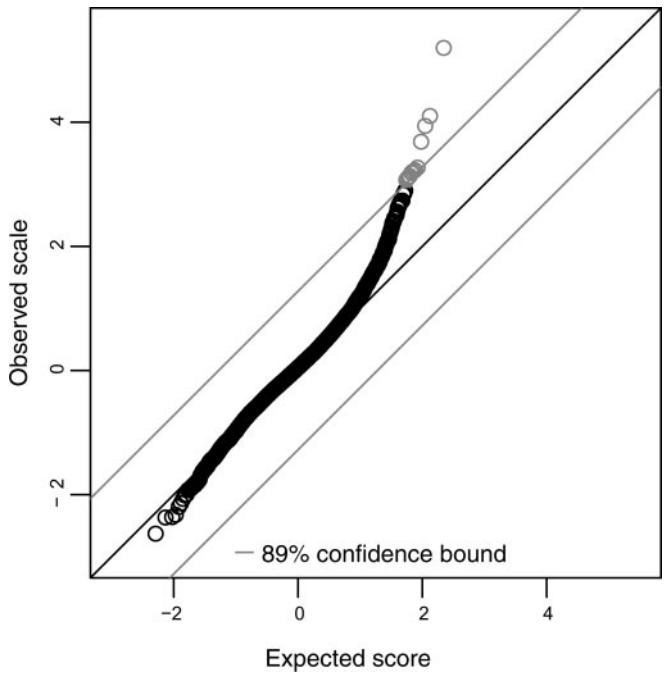

Fig. 2. Observed versus expected Z scores (significant analysis of microarray plot) in hypotensive and control animals. The solid diagonal line denotes identity between observed and expected scores. Deviation from this line indicates differential expression. The shaded lines mark the confidence area on the difference of observed to expected scores, computed from permutation scores. Scores exceeding the confidence intervals are shaded and reveal significantly differentially expressed genes.

Choosing a threshold that corresponds to the 89% confidence bound above yielded an estimated FDR of 0%. Thus we do not expect a single false positive among the set of 12 genes. The resulting estimated FDR for various choices of confidence bounds are summarized in Table 2. Details about the top 59 genes (confidence interval 25%, FDR 0.0314) are presented in Table 3, where GenBank accession numbers, Z scores, fold changes, and additional gene information are given.

In the following, we focus on the 12 genes, including 4 expressed sequence tags (ESTs), that exceeded the 89% confidence interval (Table 4 and Fig. 3). These upregulated genes were subjected to confirmation analysis. Real-time PCR experiments of the renal samples confirmed the array results in 8 of 12 cases: *Igfbp1*, *Xdh*, *Sult1a1*, *Mawbp*, *Por*, and *Gstm1* and the ESTs *BI277460* and *AI411345* (Table 4).

Because four of the eight genes affect the metabolism of ROS, we carried out an assessment of endothelial function in the rat thoracic aorta. PE (1 μmol/l) induced a maximum vasoconstriction of 14.0 ± 1.0 mN in normotensive rats and 14.1 ± 1.1 mN in hypotensive rats (not significant, $n = 6$ each). The addition of ACh (1 nmol/l–100 μmol/l) induced NO-dependent relaxations of the vessels. The vasodilatory effect of ACh was concentration dependent (Fig. 4, *A–C*). Maximum ACh-induced vasodilations (100 μmol/l) were significantly ($P < 0.05$, $n = 6$) lower in the hypotensive group (5.4 ± 0.8 mN according to 38.3 ± 5.7% of maximal vasoconstriction) than in the normotensive group (12.0 ± 0.4 mN according to 85.7 ± 2.9% of maximal vasoconstriction). The EC_{50} (log mol/l) of ACh was 6.3 ± 0.3 in the normotensive group and 5.4 ± 0.1 in the hypotensive group, indicating a significant ($P < 0.05$, $n = 6$) shift to the right of the dose-response curve (Fig. 4*C*). The direct vasodilator agent SNP (1 μmol/l) evoked comparable maximal relaxations in the two groups without any significant difference (normotensive rats: 14.1 ± 0.2 mN vs. hypotensive rats: 14.2 ± 0.2 mN, $n = 6$, data not shown). In the presence of the superoxide scavenger tiron, ACh-induced relaxations (1 mmol/l, $P < 0.05$, $n = 6$) were significantly increased in hypotensive rats, from 5.4 ± 0.8 to 8.9 ± 1.2 mN, but were principally unchanged in the control group (control: 12.0 ± 0.4; control + tiron: 12.0 ± 0.6

Table 3. *Genes exceeding the 25% confidence bound in the microarray analysis*

Gene	Accession No.	*Z* Score	Fold Change	Biological Function	Description
Sqstm1	BF400606	5.20	2.10	Transcription cofactor	Sequestosome 1
Por	NM_031576	4.10	1.58	Electron transport	Cytochrome *P*-450 oxidoreductase
Xdh	NM_017154	3.94	1.67	Electron transport	Xanthine dehydrogenase similar to proline oxidase; PRODH
EST	AI411345	3.69	1.62		
Igfbp1	NM_013144	3.18	1.90	Regulation of cell growth	Insulin-like growth factor binding protein 1
Sult1a1	AF394783	3.09	1.69	Drug metabolism	Sulfotransferase family 1A, phenol-preferring, member 1
Mawbp	AY083160	3.23	1.39	Biosynthesis	MAWD binding protein
Akr1b8	AI233740	3.07	1.62	NA	Aldo-keto reductase family 1, member B8
EST	BI277460	3.21	1.81	NA	Highly similar to phosphoenolpyruvate carboxykinase 1
EST	BM386079	3.11	1.25	NA	Similar to kinesin-like 8
EST	BE329273	3.13	1.45	Gluconeogenesis, glycerol synthesis	Highly similar to 6-phosphofructo-2-kinase/fructose-2,6-biphosphatase 4
Gstm1	M28241	3.27	1.49	Production of antioxidants	Glutathione *S*-transferase-μ_1
Dsipi	NM_031345	2.85	1.56	Fluid secretion	δ-Sleep-inducing peptide, immunoreactor
Atox1	NM_053359	2.67	1.23	Copper ion homeostasis	Antioxidant protein 1 homolog 1 (yeast)
Ddit3	NM_024134	2.62	1.39	Regulation of transcription	DNA damage-inducible transcript 3
Hmox1	NM_012580	2.73	1.71	Heme oxidation	Heme oxygenase 1
EST	BI278288	2.71	1.28	NA	Similar to RIKEN cDNA 0610039C21
EST	BI294778	2.67	1.39	NA	Similar to RIKEN cDNA 0610011L13
EST	BM387041	2.72	1.31	NA	NA
S100a9	NM_053587	2.90	1.43	Calcium ion binding	S100 calcium-binding protein A9 (calgranulin B)
EST	BM383531	2.84	1.51	NA	NA
EST	AW534837	2.74	1.74	NA	Similar to FK 506 binding protein 5
G6pc	NM_013098	2.62	1.50	Glycogen biosynthesis, Gluconeogenesis	Glucose-6-phosphatase, catalytic
Atf4	NM_024403	2.38	1.37	Regulation of transcription	Activating transcription factor 4
Dci	NM_017306	2.38	1.47	Fatty acid metabolism	Dodecenoyl-coenzyme A-δ isomerase
G6pc	U07993	2.39	1.48	Glycogen biosynthesis, gluconeogenesis	Glucose-6-phosphatase, catalytic
EST	AA894008	2.46	1.27	NA	Similar to protein 4,1, P4,1-mouse
Krt2-8	BF281337	2.45	1.23	Cytoskeleton organization	Keratin complex 2, basic, gene 8
EST	BE109381	2.36	1.36	NA	NA
Acaa1	NM_012489	2.40	1.42	Fatty acid metabolism	Acetyl-coenzyme A acyltransferase 1
Mgll	AI713204	2.47	1.35	Lipid metabolism	Monoglyceride lipase
Comt	NM_012531	2.50	1.36	Catecholamine metabolism	Catechol-*O*-methyltransferase
Pcscl	AI177358	2.51	1.76	NA	Peroxisomal Ca-dependent solute carrier-like protein
EST	AI235474	2.31	1.44	Protein kinase	NA
Ephx1	NM_012844	2.48	1.46	Proteolysis, peptidolysis	Epoxide hydrolase 1
EST	AI071166	2.56	1.53	NA	Similar to 1110007F12Rik protein
Cib1	NM_031145	2.17	1.19	Integrin-mediated	Calcium and integrin binding 1

The fold change is hypotense/normotensive. The FDR was 0.0314. NA, no data available; EST, expressed sequence tag.

mN; Fig. 4*D*). Maximal ACh-induced vasodilation was still significantly lower in hypotensive than normotensive animals ($P < 0.05$). The EC_{50} of ACh-induced vasodilation in hypotensive animals was significantly shifted to the left [hypotensive rat + tiron EC_{50} (−log mol/l): 6.4 ± 0.2 vs. hypotensive rat: 5.4 ± 0.1, $P < 0.05$, $n = 6$] in the presence of tiron but remained essentially unchanged in normotensive rats [normotensive rat + tiron EC_{50} (−log mol/l): 6.5 ± 0.4 vs. normotensive rat: 6.7 ± 0.5, $n = 6$]. SNP-induced relaxations were not significantly affected by tiron in normotensive and hypotensive rats (normotensive rats: 14.2 ± 0.4 mN vs. hypotensive rats: 14.0 ± 0.3 mN, $n = 6$, data not shown).

The eight genes that were upregulated in both microarray analysis and real-time PCR in the kidney samples were consecutively tested for differential expression in thoracic aorta samples. *Xdh*, *Mwbp, Gstm1,* and *Por* were upregulated ($P < 0.1$), whereas *Sult1a1* and *AI411345* were downregulated. *Igfbp1* and *BI277460* showed no significant differential expression (Table 4).

DISCUSSION

In the present study, we established a rodent model that constitutes a physiogenomic approach to study the regulation of blood pressure. To find new vasoregulatory mechanisms, we induced acute hypotension in normotensive rats, assuming that vasoregulatory systems will counteract hypotension.

We performed microarray analysis of rat kidneys 6 h after the initiation of acute hypotension and identified the following genes to be significantly upregulated.

Table 4. *Differentially expressed genes in microarray analysis and real-time PCR*

	Kidney Microarray analysis		Kidney Real-Time PCR		Aorta Real-time PCR		
Accession No.	Fold change	*Z* score	Fold change	*P* value	Fold change	*P* value	Gene
NM_017154	1.67	3.94	1.57	0.02	1.46	0.06	*Xdh,* xanthine dehydrogenase
NM_053405	1.58	4.1	1.59	0.04	1.66	0.07	*Por,* cytochrome P = 450 oxidoreductase
AI411345	1.62	3.69	1.6	0.07	0.59	0.004	EST, highly similar to proline oxidase, mitochondrial precursor (*M. musculus*)
NM_017014	1.49	3.27	1.79	0.03	0.66	0.0001	*Gstm1,* glutathione *S*-transferase-μ_1
NM_138530	1.39	3.23	1.41	0.03	1.75	0.008	*Mawbp,* MAWD binding protein
NM_031834	1.69	3.09	1.36	0.08	0.75	0.03	*Sult1a1,* sulfotransferase family 1A, phenol-preferring, member 1
NM_013144	1.90	3.18	1.73	0.08	0.72	0.67	*Igfbp1,* insulin-like growth factor binding protein 1
BI277460	1.81	3.21	2.81	0.01	1.29	0.57	EST, highly similar to phosphoenolpyruvate carboxykinase 1
AI233740	1.62	3.07	1.6	0.24	ND	ND	*Akr1b8,* aldo-keto reductase family 1, member B8
BM386079	1.25	3.11	1.07	0.59	ND	ND	EST, similar to kinesin-like 8
BF400606	2.10	5.20	0.78	0.47	ND	ND	*Sqstm1,* sequestosome 1
BE329273	1.45	3.13	1.15	0.55	ND	ND	EST, highly similar to 6-phosphofructo-2-kinase/fructose-2,6-biphosphatase 4

Genes exceeding the 89% confidence interval bound in the microarray analysis are shown. The fold change is hypotensive/normotensive. ND, not done.

Xdh encodes for xanthine oxidoreductase, a molybdoenzyme capable of catalyzing the oxidation of hypoxanthine and xanthine in the process of purine metabolism. Xanthine oxidoreductase can exist in two interconvertible forms, either as xanthine dehydrogenase (XD) or xanthine oxidase (XO) (24). The former reduces NAD^+, whereas the latter prefers molecular oxygen as a substrate, leading to the production of the potent vasoconstrictors O_2^- and H_2O_2 (7). XD and XO are expressed at high levels on the luminal surface of the endothelium (2). XO-derived O_2^- generation has been repeatedly demonstrated in cardiovascular disease including endothelial dysfunction, in heavy smokers (12), and in hypercholesterolemia (2, 27).

Por encodes for NADPH-cytochrome *P*-450 oxidoreductase, a part of the membrane-bound cytochrome *P*-450 multienzyme system. At present, there is increasing evidence that cytochrome *P*-450 metabolites of arachidonic acid play an important role in vasoregulation and renal function by depolarizing vascular smooth muscle cells and modulating renal sodium reabsorption (31). Furthermore, vascular cytochrome *P*-450 monooxygenases have been identified as a source of ROS (8, 9). O_2^-, H_2O_2, and hydroxyl radicals can be generated during the cytochrome *P*-450 reaction cycle, when the electrons needed for reducing the central heme iron are transferred to the activated bound oxygen molecule.

The EST *AI411345* is highly similar (99%) to mouse proline oxidase. Proline oxidase is a mitochondrial enzyme catalyzing the conversion of proline to pyrroline-5-carboxylate with the concomitant transfer of electrons to cytochrome *c*. Proline oxidase can generate proline-dependent ROS (5).

Glutathione *S*-transferases protect various cell types including vascular smooth muscle cells and endothelial cells against oxidant damage (41). The Atherosclerosis Risk in Communities study demonstrated that *Gtsm1* polymorphisms modify the effect of smoking on endothelial function and atherosclerosis (25). Thus smokers having the null genotype of GSTM1 are at a higher risk for developing coronary heart disease (36). ROS induce glutathione *S*-transferases by antioxidant response elements (16). Interestingly, *Gstm1* is downregulated in stroke-prone spontaneously hypertensive rats (SHR), leading to increased oxidative stress (22).

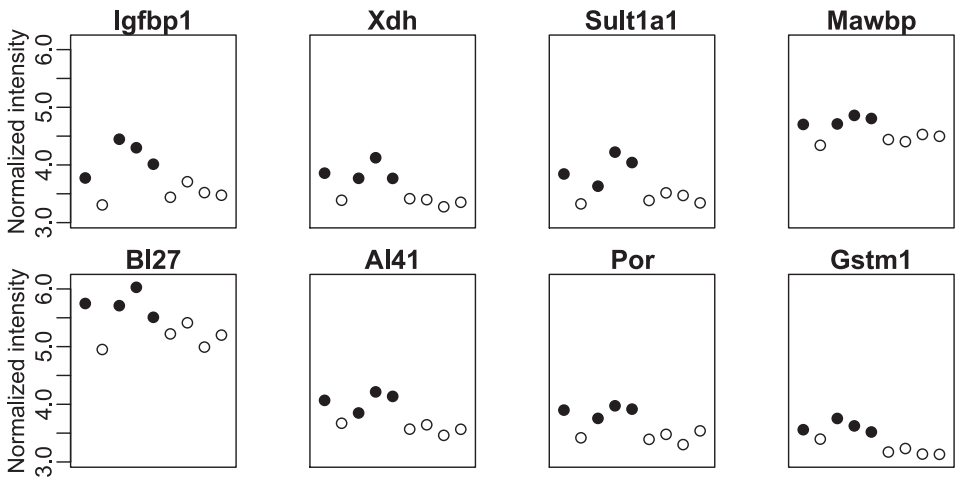

Fig. 3. Normalized intensity values of differentially expressed genes in the microarray analysis. *y*-Axes with expression values on the transformed scale are identical for all plots. Solid circles denote case samples; open circles denote control samples. Order of samples corresponds to the chronology of hybridization.

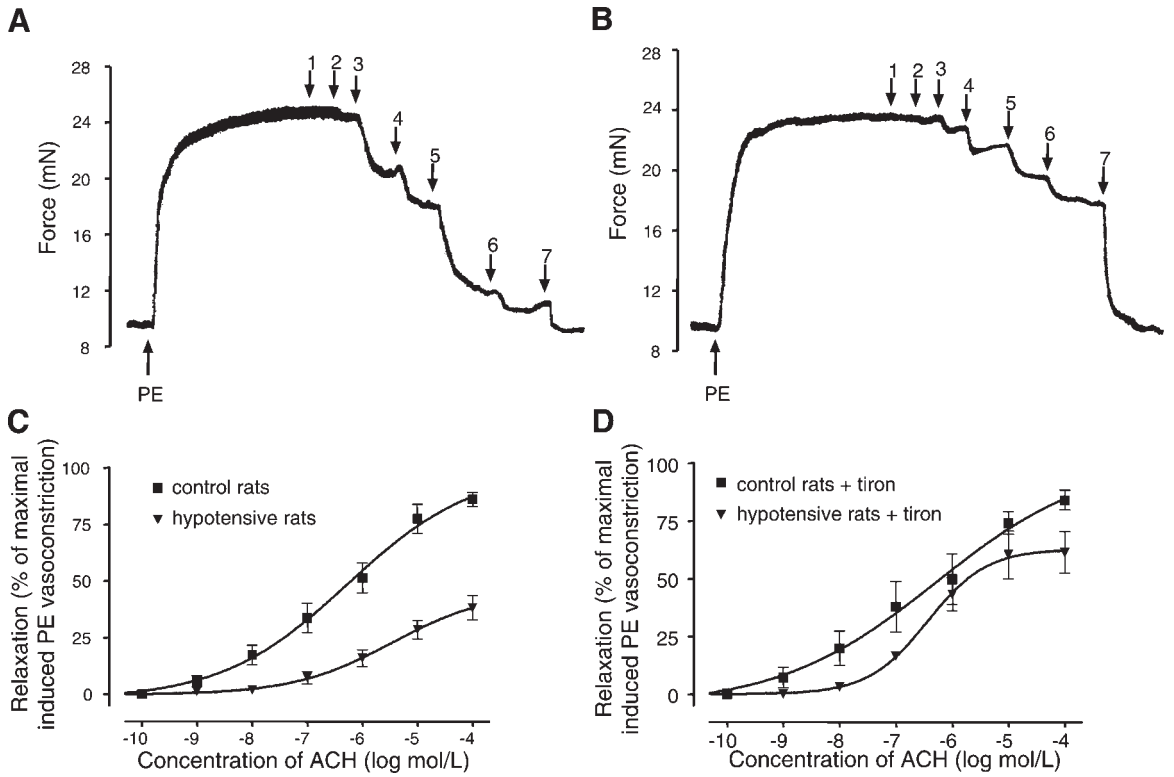

Fig. 4. Acetylcholine (ACh)-induced vasodilation in aortae from control and hypotensive rats. *A* and *B*: thoracic aortic rings from control (*A*) and hypotensive (*B*) rats were precontracted with phenylephrine (PE; 1 μmol/l), and direct relaxation responses to ACh in ascending concentrations (*1*, 1 nmol/l; *2*, 10 nmol/l; *3*, 100 nmol/l; *4*, 1 μmol/l; *5*, 10 μmol/l; and *6*, 100 μmol/l ACh and *7*, 1 μmol/l sodium nitroprusside) were measured. Shown are representative tracings from one typical experiment out of six each. *C*: cumulative findings (means ± SE) for dose-dependent relaxation to ACh in PE-precontracted aortae from control and hypotensive animals ($n = 6$). *D*: cumulative findings (means ± SE) for dose-dependent relaxation to ACh in PE-precontracted aortae from control and hypotensive animals in the presence of the radical scavenger tiron (1 mmol/l, $n = 6$).

Mawbp encodes for MAWD binding protein. The recently discovered protein MAWD is structurally characterized by WD-40 repeats and is frequently overexpressed in breast cancer(21). At present, it has no known function in the cardiovascular system.

Cytosolic sulfotransferases catalyze sulfoconjugation of small lipophilic endobiotics and xenobiotics. At least 44 cytosolic sulfotransferases have been identified from mammals, including sulfotransferase 1 type A_1 (*Sult1a1*) (11). None of them is known to play a role in the cardiovascular system.

Insulin-like growth factor (IGF-I) is an essential regulator of developmental growth. Moreover, there is an increasing body of evidence demonstrating that IGF-I exerts multiple vascular effects through endocrine, autocrine, and paracrine mechanisms (3). Because IGF-I induces NO production in endothelial cells, it is a potent mediator of vasodilation (38) and is capable of lowering systemic blood pressure (30). IGF binding protein 1 (IGFBP1) is a carrier protein that binds to IGF-I with high affinity and therefore is placed in a critical regulatory position between IGF-I and its receptor.

The EST *BI277460* is highly similar to phosphoenolpyruvate carboxykinase (PEPCK), which is not reported to have cardiovascular effects. However, strikingly, there are remarkable similarities between IGFBP1 and the PEPCK promoter (19), including regions conferring insulin, glucocorticoids, and cAMP responses.

In summary, four of six functionally known upregulated genes are known to play a role in the cardiovascular system. Three of the corresponding proteins affect the metabolism of ROS. Xanthine oxidoreductase, vascular cytochrome *P*-450 monooxygenases, and possibly the protein highly similar to proline oxidase are capable of generating ROS. It may be speculated that glutathione *S*-transferase is compensatorily overexpressed due to the increased levels of ROS.

Both endothelial and vascular smooth muscle cells produce ROS from a variety of enzymatic sources including NADPH oxidase, XO, and NO synthases (NOSs) (37). Accumulating evidence suggests that oxidant stress alters many functions of the endothelium, including modulation of vasomotor tone. Inactivation of NO by superoxide and other reactive oxygen compounds leads to a decreased vasodilator potency, which is commonly referred to as endothelial dysfunction (20). In our experiments, three of six functionally known upregulated genes and eventually one of two upregulated ESTs affect the metabolism of ROS. Therefore, we investigated a possible compensatory alteration of endothelial function by means of arterial relaxation studies with aortic rings. Indeed, vasodilator potency was largely diminished 6 h after the intitiation of acute hypotension. Because only ACh-induced vasodilations were reduced, whereas SNP-induced vasodilations were equivalent, in aortae of normo- and hypotensive animals, the observed effect is due to a decreased bioavailability of NO. Decreased endothelial NO availability may be caused by decreased expression of endothelial NOS (eNOS), a lack of substrate, or cofactors for eNOS, alterations of cellular signaling such that eNOS is not appropriately activated, and, finally, accelerated

NO degradation by ROS. Because the vasodilator potency of the endothelium was partially restored by the superoxide scavenger tiron in our experiments, the reduction of NO bioavailability was a consequence of NO degradation by ROS.

For practical reasons, arterial relaxation studies were performed in aortae. Counteracting vasoregulatory mechanisms vary in different vascular beds. Vasoconstriction is more prominent in smaller resistance arteries than in large elastic vessels like the aorta. Further studies will have to provide a detailed characterization of endothelial counterregulation in hypotension in different vascular beds.

In analogy to renal tissue, real-time PCR results from aortic tissue show that the expression of the two ROS-producing enzymes *Xdh* and *Por* is increased in hypotension as well. Because kidney samples consist of a variety of parenchymal structures including interstitial tissue, the tubular system, glomeruli, and vessels, it is not surprising that for some genes (*Sult1a1*, *AI411345*, *Igfbp1*, and *BI277460*), the direction of changes in expression was not consistent in the kidney and aorta.

Currently, increased inactivation of NO by O_2^- and other ROS is regarded as a companion of pathological conditions such as hypertension, hypercholesterolemia, diabetes, and cigarette smoking (2). Our data suggest that ROS-mediated control of endothelial NO availability can contribute to the physiological regulation of vascular tone as well. XO-derived O_2^- has been reported to contribute to impaired endothelium-dependent vasodilatation and increased blood pressure in SHR (34). Activation of vascular cytochrome *P*-450 leads to an increase in the generation of O_2^- and plays an important role in hypertension (32). Our data suggest that NADPH-cytochrome *P*-450 oxidoreductase might play a critical role in the regulation of vascular cytochrome *P*-450.

The methodology of microarray analysis offers a promising possibility of gaining insight into the genetics of hypertension. In the present study, this technology led to the detection of a ROS-mediated endothelial dysfunction counteracting arterial hypotension. However, expression analysis comparing WKY with SHR failed to identify candidate genes for the control of blood pressure (28). SHR are derived from hypertensive WKY rats, but the two strains are genetically heterogeneous. It may be speculated that the genetic identity of case and control animals constitutes the crucial advantage of our model. In diabetes research, Kim and coworkers (18) established an experimental design that shows similarities to our approach. They induced acute hypoglycemia in mice to increase the expression of counteracting genes that might mediate a raise of blood glucose (18). Microarray analysis revealed the gene that is now called *resistin* (33).

The present work links a further group of functionally related genes to the genetic basis of blood pressure regulation. Further studies will have to reveal which is the afferent loop that detects hypotension and generates the signaling necessary to achieve the coordinated upregulation of several oxidative genes. Is the sensor located in large vessels, directly detecting changes in wall tension, or is it located in microvessels or tissues, detecting metabolic changes due to hypoperfusion?

In summary, the present large-scale genome screening model is capable of detecting vasoregulatory mechanisms. The study is limited by the fact that only one particular time is analyzed after the initiation of hypotension. Further transcriptome analyses at different times will allow a distinction between acute and long-term phenomena and between regulatory and compensatory counterbalancing mechanisms. This physiogenomic approach may provide deeper insight into the genetics and physiology of blood pressure regulation.

ACKNOWLEDGMENTS

We thank the German Genome Resource Center Berlin for the support in array hybridization. We thank I. Dunkel (Max-Planck Institute for Molecular Genetics) for technical assistance.

REFERENCES

1. **Bunag RD.** Validation in awake rats of a tail-cuff method for measuring systolic pressure. *J Appl Physiol* 34: 279–282, 1973.
2. **Cai H and Harrison DG.** Endothelial dysfunction in cardiovascular diseases: the role of oxidant stress. *Circ Res* 87: 840–844, 2000.
3. **Delafontaine P, Song YH, and Li Y.** Expression, regulation, and function of IGF-1, IGF-1R, and IGF-1 binding proteins in blood vessels. *Arterioscler Thromb Vasc Biol* 24: 435–444, 2004.
4. **Dietz R, Schomig A, Haebara H, Mann JF, Rascher W, Luth JB, Grunherz N, and Gross F.** Studies on the pathogenesis of spontaneous hypertension in rats. *Circ Res* 43: I98-I106, 1978.
5. **Donald SP, Sun XY, Hu CA, Yu J, Mei JM, Valle D, and Phang JM.** Proline oxidase, encoded by p53-induced gene-6, catalyzes the generation of proline-dependent reactive oxygen species. *Cancer Res* 61: 1810–1815, 2001.
6. **Efron B and Tibshirani R.** Empirical bayes methods and false discovery rates for microarrays. *Genet Epidemiol* 23: 70–86, 2002.
7. **Ellis A and Triggle CR.** Endothelium-derived reactive oxygen species: their relationship to endothelium-dependent hyperpolarization and vascular tone. *Can J Physiol Pharmacol* 81: 1013–1028, 2003.
8. **Fleming I.** Cytochrome p450 and vascular homeostasis. *Circ Res* 89: 753–762, 2001.
9. **Fleming I, Michaelis UR, Bredenkotter D, Fisslthaler B, Dehghani F, Brandes RP, and Busse R.** Endothelium-derived hyperpolarizing factor synthase (cytochrome P450 2C9) is a functionally significant source of reactive oxygen species in coronary arteries. *Circ Res* 88: 44–51, 2001.
10. **Gentleman RC, Carey VJ, Bates DM, Bolstad B, Dettling M, Dudoit S, Ellis B, Gautier L, Ge Y, Gentry J, Hornik K, Hothorn T, Huber W, Iacus S, Irizarry R, Leisch F, Li C, Maechler M, Rossini AJ, Sawitzki G, Smith C, Smyth G, Tierney L, Yang JY, and Zhang J.** Bioconductor: open software development for computational biology and bioinformatics. *Genome Biol* 5: R80, 2004.
11. **Glatt H.** Sulfotransferases in the bioactivation of xenobiotics. *Chem Biol Interact* 129: 141–170, 2000.
12. **Guthikonda S, Sinkey C, Barenz T, and Haynes WG.** Xanthine oxidase inhibition reverses endothelial dysfunction in heavy smokers. *Circulation* 107: 416–421, 2003.
13. **Huber W, von Heydebreck A, Sultmann H, Poustka A, and Vingron M.** Variance stabilization applied to microarray data calibration and to the quantification of differential expression. *Bioinformatics* 18, *Suppl* 1: S96–S104, 2002.
14. **Ihaka R and Gentleman RC.** R: a language for data analysis and graphics. *J Comp Graph Stat* 5: 299–314, 1996.
15. **Irizarry RA, Bolstad BM, Collin F, Cope LM, Hobbs B, and Speed TP.** Summaries of Affymetrix GeneChip probe level data. *Nucleic Acids Res* 31: e15, 2003.
16. **Kang KW, Choi SH, and Kim SG.** Peroxynitrite activates NF-E2-related factor 2/antioxidant response element through the pathway of phosphatidylinositol 3-kinase: the role of nitric oxide synthase in rat glutathione *S*-transferase A2 induction. *Nitric Oxide* 7: 244–253, 2002.
17. **Katusic ZS and Vanhoutte PM.** Superoxide anion is an endothelium-derived contracting factor. *Am J Physiol Heart Circ Physiol* 257: H33–H37, 1989.
18. **Kim KH, Lee K, Moon YS, and Sul HS.** A cysteine-rich adipose tissue-specific secretory factor inhibits adipocyte differentiation. *J Biol Chem* 276: 11252–11256, 2001.
19. **Lee PD, Giudice LC, Conover CA, and Powell DR.** Insulin-like growth factor binding protein-1: recent findings and new directions. *Proc Soc Exp Biol Med* 216: 319–357, 1997.

20. **Li JM and Shah AM.** Endothelial cell superoxide generation: regulation and relevance for cardiovascular pathophysiology. *Am J Physiol Regul Integr Comp Physiol* 287: R1014–R1030, 2004.
21. **Matsuda S, Katsumata R, Okuda T, Yamamoto T, Miyazaki K, Senga T, Machida K, Thant AA, Nakatsugawa S, and Hamaguchi M.** Molecular cloning and characterization of human MAWD, a novel protein containing WD-40 repeats frequently overexpressed in breast cancer. *Cancer Res* 60: 13–17, 2000.
22. **McBride MW, Brosnan MJ, Mathers J, McLellan LI, Miller WH, Graham D, Hanlon N, Hamilton CA, Polke JM, Lee WK, and Dominiczak AF.** Reduction of Gstm1 expression in the stroke-prone spontaneously hypertension rat contributes to increased oxidative stress. *Hypertension* 45: 786–792, 2005.
23. **McGiff JC and Quilley J.** 20-Hydroxyeicosatetraenoic acid and epoxyeicosatrienoic acids and blood pressure. *Curr Opin Nephrol Hypertens* 10: 231–237, 2001.
24. **Meneshian A and Bulkley GB.** The physiology of endothelial xanthine oxidase: from urate catabolism to reperfusion injury to inflammatory signal transduction. *Microcirculation* 9: 161–175, 2002.
25. **Miller EA, Pankow JS, Millikan RC, Bray MS, Ballantyne CM, Bell DA, Heiss G, and Li R.** Glutathione-*S*-transferase genotypes, smoking, and their association with markers of inflammation, hemostasis, and endothelial function: the Atherosclerosis Risk in Communities (ARIC) study. *Atherosclerosis* 171: 265–272, 2003.
26. **Nofer JR, van der Giet M, Tolle M, Wolinska I, von Wnuck Lipinski K., Baba H.A, Tietge UJ, Godecke A, Ishii I, Kleuser B, Schafers M, Fobker M, Zidek W, Assmann G, Chun J, and Levkau B.** HDL induces NO-dependent vasorelaxation via the lysophospholipid receptor S1P3. *J Clin Invest* 113: 569–581, 2004.
27. **Ohara Y, Peterson TE, and Harrison DG.** Hypercholesterolemia increases endothelial superoxide anion production. *J Clin Invest* 91: 2546–2551, 1993.
28. **Okuda T, Sumiya T, Mizutani K, Tago N, Miyata T, Tanabe T, Kato H, Katsuya T, Higaki J, Ogihara T, Tsujita Y, and Iwai N.** Analyses of differential gene expression in genetic hypertensive rats by microarray. *Hypertens Res* 25: 249–255, 2002.
29. **Palmer RM, Ferrige AG, and Moncada S.** Nitric oxide release accounts for the biological activity of endothelium-derived relaxing factor. *Nature* 327: 524–526, 1987.
30. **Pete G, Hu Y, Walsh M, Sowers J, and Dunbar JC.** Insulin-like growth factor-I decreases mean blood pressure and selectively increases regional blood flow in normal rats. *Proc Soc Exp Biol Med* 213: 187–192, 1996.
31. **Roman RJ.** P-450 metabolites of arachidonic acid in the control of cardiovascular function. *Physiol Rev* 82: 131–185, 2002.
32. **Sarkis A, Lopez B, and Roman RJ.** Role of 20-hydroxyeicosatetraenoic acid and epoxyeicosatrienoic acids in hypertension. *Curr Opin Nephrol Hypertens* 13: 205–214, 2004.
33. **Steppan CM, Bailey ST, Bhat S, Brown EJ, Banerjee RR, Wright CM, Patel HR, Ahima RS, and Lazar MA.** The hormone resistin links obesity to diabetes. *Nature* 409: 307–312, 2001.
34. **Suzuki H, DeLano FA, Parks DA, Jamshidi N, Granger DN, Ishii H, Suematsu M, Zweifach BW, and Schmid-Schonbein GW.** Xanthine oxidase activity associated with arterial blood pressure in spontaneously hypertensive rats. *Proc Natl Acad Sci USA* 95: 4754–4759, 1998.
35. **Suzuki H and Saruta T.** An overview of blood pressure regulation associated with the kidney. *Contrib Nephrol* 143: 1–15, 2004.
36. **Tamer L, Ercan B, Camsari A, Yildirim H, Cicek D, Sucu N, Ates NA, and Atik U.** Glutathione *S*-transferase gene polymorphism as a susceptibility factor in smoking-related coronary artery disease. *Basic Res Cardiol* 99: 223–229, 2004.
37. **Taniyama Y and Griendling KK.** Reactive oxygen species in the vasculature: molecular and cellular mechanisms. *Hypertension* 42: 1075–1081, 2003.
38. **Tsukahara H, Gordienko DV, Tonshoff B, Gelato MC, and Goligorsky MS.** Direct demonstration of insulin-like growth factor-I-induced nitric oxide production by endothelial cells. *Kidney Int* 45: 598–604, 1994.
39. **Tusher VG, Tibshirani R, and Chu G.** Significance analysis of microarrays applied to the ionizing radiation response. *Proc Natl Acad Sci USA* 98: 5116–5121, 2001.
40. **Yanagisawa M, Kurihara H, Kimura S, Tomobe Y, Kobayashi M, Mitsui Y, Yazaki Y, Goto K, and Masaki T.** A novel potent vasoconstrictor peptide produced by vascular endothelial cells. *Nature* 332: 411–415, 1988.
41. **Yang Y, Yang Y, Trent MB, He N, Lick SD, Zimniak P, Awasthi YC, and Boor PJ.** Glutathione-*S*-transferase A4–4 modulates oxidative stress in endothelium: possible role in human atherosclerosis. *Atherosclerosis* 173: 211–221, 2004.